THE ASTROPHYSICAL JOURNAL, 364:555–560, 1990 December 1

95 GHz METHANOL MASERS NEAR DR 21 AND DR 21(OH)

R. L. PLAMBECK
Radio Astronomy Laboratory, University of California, Berkeley
AND
K. M. MENTEN
Harvard-Smithsonian Center for Astrophysics
Received 1990 March 26; accepted 1990 June 1

ABSTRACT

We used the BIMA array to map the 95 GHz $8_0 \rightarrow 7_1A^+$ transition of methanol and the 98 GHz $J = 2 \rightarrow 1$ transition of CS toward the DR 21(OH) and DR 21 star-forming regions. Several strong methanol masers were found. The positions of the two brightest masers were measured with an accuracy of about $\pm 0\farcs3$. Toward DR 21(OH), the positions, velocities, and line shapes of the 95 GHz masers are in excellent agreement with those of the 84 GHz $5_{-1} \rightarrow 4_0 E$ methanol masers previously mapped by Batrla and Menten, demonstrating that maser emission in both transitions originates from the same clumps of gas. The methanol masers are offset from CS emission peaks and from other known infrared and maser sources; they may possibly be clustered along the interface between outflows, traced by shock-excited H_2 emission, and dense ambient gas, traced by CS emission.

Subject headings: interstellar: molecules — masers — nebulae: H II regions — nebulae: individual (DR 21) — radiation mechanisms

I. INTRODUCTION

Interstellar methanol (CH_3OH) masers are observed in two distinctly different environments. A number of methanol transitions, most prominently the strong 12 GHz $2_0 \rightarrow 3_{-1}E$ line (Batrla *et al.* 1987), show maser action toward compact H II regions, like W3(OH). These so-called *class B* methanol masers share many of the properties of the OH masers associated with these sources. In contrast, *class A* methanol masers are typically far offset from OH and H_2O masers, known infrared and radio-continuum sources, and other molecular emission peaks. The hitherto detected transitions from these masers are the $4_{-1} \rightarrow 3_0 E$, $7_0 \rightarrow 6_1A^+$, $5_{-1} \rightarrow 4_0 E$, and $8_0 \rightarrow 7_1A^+$ lines at 36, 44, 84, and 95 GHz, as well as the series of $J_{k=2} \rightarrow J_{k=1}E$ ($J = 2, 3, 4\ldots$) transitions near 25 GHz. Spectra of two or more class A methanol transitions toward the same maser position frequently show a striking resemblance to one another—usually a single strong spike is observed at the same LSR velocity—suggesting that all the lines are emitted from the same volume of gas.

Accurate position measurements are needed in order to make further progress in understanding the class A masers. Such measurements are necessary to confirm that masers in different transitions originate from exactly the same spot, in order to constrain models of the maser mechanism. In addition, accurate position measurements will allow sensitive searches for deeply embedded infrared sources coincident with the masers. To date, only a few interferometric observations of class A masers have been made: toward Orion-KL at 25 GHz (Matsakis *et al.* 1980; Johnston *et al.* 1990) and 95 GHz (Plambeck and Wright 1988), and toward DR 21(OH) at 84 GHz (Batrla and Menten 1988).

In this paper we report aperture synthesis observations of the $8_0 \rightarrow 7_1A^+$ transition of methanol toward the DR 21 and DR 21(OH) (also known as W75 S) star-forming regions, both of which show maser emission from other methanol transitions. Observations of the $J = 2 \rightarrow 1$ transition of CS were made simultaneously, providing maps of the dense molecular cores in the neighborhood of the masers.

II. OBSERVATIONS

Data were obtained at four configurations of the BIMA array[1] at the Hat Creek Radio Observatory between 1989 January and May. Projected antenna spacings ranged from 2 kλ to 27 kλ. At 95 GHz, the three 6.1 m diameter antennas have primary beamwidths of $\sim 2\farcm1$. We interleaved observations of two fields, one centered about $1\farcm1$ W of the DR 21 continuum source, the other near DR 21(OH); Figure 1 indicates the positions of the two fields relative to nearby continuum and maser sources. The quasar 2037+511 was used as the phase and amplitude calibrator. Its flux density at the time of the observations was 2.9 Jy, determined by comparison with planets.

The $8_0 \rightarrow 7_1A^+$ transition of CH_3OH at rest frequency 95.169489 GHz (De Lucia *et al.* 1989) and the $2 \rightarrow 1$ transition of CS at 97.98097 GHz were observed simultaneously, in the lower and upper receiver sidebands. Signals from the two sidebands were separated by phase switching the first local oscillator. Spectra were obtained with a 512 channel cross-correlation spectrometer, configured to give a velocity resolution of 0.12 km s^{-1} over an LSR velocity range of -17 to $+11$ km s^{-1}.

The data were mapped and CLEANed using the RALINT data reduction package developed at the University of California at Berkeley. The synthesized beamwidth was approximately $6\farcs5 \times 4\farcs4$. The rms noise in individual 0.12 km^{-1} wide velocity channels was 1.7 Jy per beam. The maps are insensitive to structures larger than about 50″ in size.

[1] Operated by the University of California at Berkeley, the University of Illinois, and the University of Maryland, with support from the National Science Foundation.

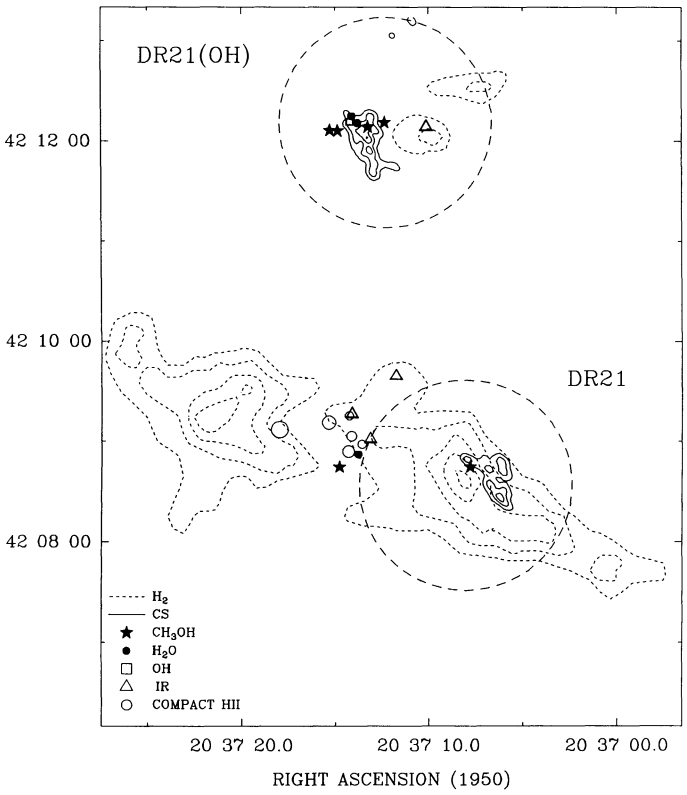

FIG. 1.—Overview of the DR 21/DR 21(OH) region. Dashed circles indicate the two fields mapped with the BIMA array; the circles are 2.1 in diameter, equal to the primary beamwidths of the BIMA antennas. The phase-tracking centers were $\alpha_{1950} = 20^h37^m08^s.065$, $\delta_{1950} = 42°08'34''$, about 1.1 W of the DR 21 continuum source; and $\alpha_{1950} = 20^h37^m12^s.3$, $\delta_{1950} = 42°12'11''$, coincident with the strongest DR 21(OH) 84 GHz methanol maser measured by Batrla and Menten (1988). Stars denote $8_0 \rightarrow 7_1A^+$ methanol masers (this work); filled black circles indicate water maser positions (Genzel and Downes 1977). The OH masers associated with DR 21(OH) are clustered within the area delimited by the square (Norris *et al.* 1982) and are coincident with a far-infrared source (Harvey, Campbell, and Hoffman 1977). Infrared sources detected by Wynn-Williams, Becklin, and Neugebauer (1974) are marked by open triangles. Open circles denote the positions and approximate sizes of the compact DR 21 continuum sources identified by Roelfsema, Goss, and Geballe (1989). Short dashed contours represent the 2.2 μm emission from shock-excited H_2 (Garden *et al.* 1986). Solid contours indicate integrated intensity CS $J = 2 \rightarrow 1$ emission (this work). The CS contour values are 40, 80, and 120 K km s^{-1} toward DR 21(OH) and 24, 48, and 72 K km s^{-1} toward DR 21.

III. RESULTS

a) *Methanol Maser Features*

We identified four methanol maser spots in the DR 21(OH) field and two in the DR 21 field. Table 1 lists the maser positions and line parameters, while Figure 2 displays spectra generated from the maps. The absolute positions of the two strongest masers, DR 21(OH)-1 and DR 21-W, are uncertain by about 0.3 due to uncertainties in calibrating the instrumental passband. Positions of the weaker masers are uncertain by 1″–2″ owing to confusion from extended methanol emission. The maser positions are indicated in Figure 1. The maser detected just south of the DR 21 continuum peak is located 75″ from the center of the field, beyond the ~65″ half-power radius of the primary beam; the amplitude of this feature has therefore been corrected upward by a factor of 2.5 in Table 1.

The strongest maser feature, DR 21(OH)-1, has a brightness temperature of 760 K in the 6.5 × 4.4 synthesized beam. This maser spot is at most 5% broader than the synthesized beam in our maps, indicating that its true angular diameter is less than 2″, and its true brightness temperature is greater than 5000 K.

b) *Broad Methanol Emission Pedestals*

From the spectra in Figure 2, one can see that all the narrow maser features are associated with underlying emission pedestals, typically with widths of 2–3 km s^{-1} and brightness temperatures of 50 K. It is uncertain whether these broad features are attributable to maser or to thermal emission. Maps of the pedestal emission features toward DR 21(OH)-1, DR 21(OH)-2, and DR 21-W show that these features are unresolved by our beam. There is some indication, however, that the centers of the pedestal emission regions are offset by 1″–2″ from the associated maser spikes. The situation is less clear-cut toward DR 21(OH)-3 and DR 21(OH)-4; here the −5 km s^{-1} emission component is clearly resolved, with an extent of 5″ × 15″.

The four maser spots in DR 21(OH) appear to be connected by a ridge of extended, probably thermal, methanol emission. The spectrum of this component, midway between maser spots 2 and 4, is shown in Figure 5; a CS spectrum toward the same position is shown for comparison. Emission from the center of the CS line is resolved out by the interferometer or is absorbed by cooler foreground gas, but the CS and CH_3OH line wings match closely. The CH_3OH brightness temperature is 10–15 K. We do not detect 95 GHz CH_3OH emission near (α, $\delta)_{1950} = 20^h37^m14^s.0$, 42°11′25″, where Batrla and Menten

TABLE 1

POSITIONS AND LINE PARAMETERS OF $8_0 \rightarrow 7_1A^+$ CH_3OH MASERS

Component	α_{1950}[a]	δ_{1950}[a]	T_b[b] (K)	v_{LSR}[c] (km s^{-1})	Δv[c] (km s^{-1})
DR 21(OH)-1	$20^h37^m12^s.34$	42°12′11.″3	760	0.32	0.66
DR 21(OH)-2	20 37 13.23	42 12 08.6	220	0.07	0.45
DR 21(OH)-3	20 37 15.27	42 12 06.5	110	−5.3	0.5
DR 21(OH)-4	20 37 14.85	42 12 06.3	50	−6.7	0.4
DR 21-W	20 37 07.82	42 08 44.6	650	−2.52	0.4
DR 21-C	20 37 14.80	42 08 44.5	210[d]	−3.5	0.3

[a] Absolute position accuracy is about ±0.3 for DR 21(OH)-1 and DR 21-W, and 1″–2″ for other features.

[b] T_b is the brightness temperature in a 6.5 × 4.4 synthesized beam. $T_b = 1$ K corresponds to a flux density of 0.23 Jy.

[c] The LSR velocity v_{LSR} and line width (FWHM) Δv were determined from Gaussian fits to the spectra.

[d] The observed value of T_b has been multiplied by 2.5 to correct for primary beam response.

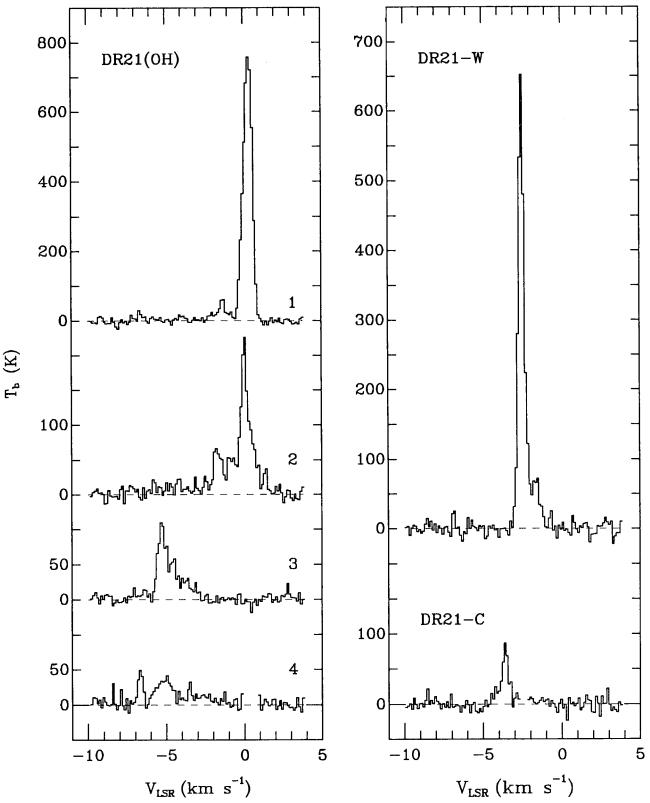

FIG. 2.—Spectra of $8_0 \rightarrow 7_1 A^+$ methanol masers detected toward DR 21(OH) and DR 21, generated from channel maps with 0.12 km s^{-1} spectral resolution and a 6″.5 × 4″.4 synthesized beam. For this beam size, a brightness temperature of 1 K corresponds to a flux density of 0.23 Jy. Note that the intensity scale for maser DR 21(OH)-1 has been compressed by a factor of 2. The intensity scale for maser DR 21-C should be multiplied by approximately 2.5, since this maser is located outside the half-power radius of the primary beam.

(1988) detect thermal emission from the 84 GHz line at a level of 5–10 K. Our upper limit on the CH_3OH intensity from this region is about 5 K.

c) CS $J = 2 \rightarrow 1$ *Maps*

Because the velocities of the methanol masers lie within a few km s^{-1} of the ambient cloud velocities, it is difficult to make meaningful comparisons between the methanol and CS emission in narrow velocity intervals: the CS emission may be quite optically thick at these velocities, and extended CS emission is largely resolved out by the aperture synthesis observations. Thus, in Figures 3 and 4 we have chosen to compare integrated intensity CS and CH_3OH maps. The methanol masers are *not* well-correlated with CS $J = 2 \rightarrow 1$ emission peaks.

Toward DR 21(OH), the brightest CS emission coincides with a 2 cm H_2CO emission region mapped with the VLA by Johnston, Henkel, and Wilson (1984); the H_2CO spectrum shown by Johnston, Henkel, and Wilson (1984) closely resembles the CS and CH_3OH spectra in Figure 5. Since densities $\geq 10^6$ cm^{-2} are necessary to produce *emission* in the 2 cm H_2CO line, this region is clearly a high-density core.

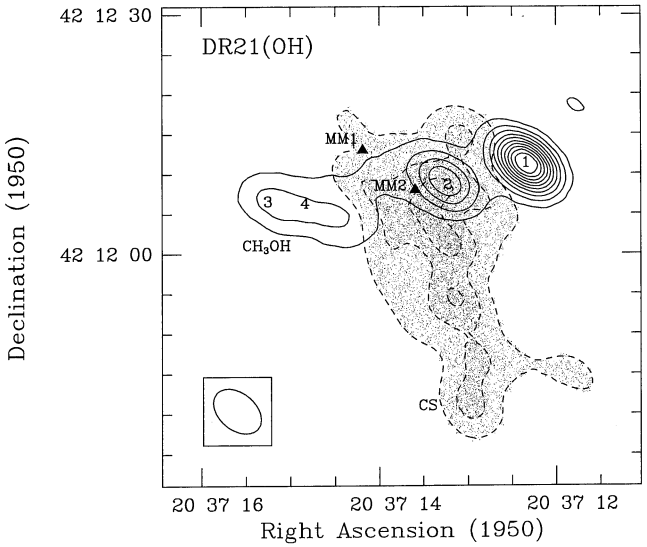

FIG. 3.—Comparison of CH_3OH $8_0 \rightarrow 7_1 A^+$ (*solid contours*) and CS $J = 2 \rightarrow 1$ (*dashed shaded contours*) integrated intensity maps toward DR 21(OH). Contours are 50, 100, ..., 500 K km s^{-1} for CH_3OH and 40, 80, and 120 K km s^{-1} for CS. Methanol maser spots are indicated by numerals 1–4. Filled triangles denote 1.4 mm continuum sources MM 1 and MM 2 mapped by Woody *et al.* (1989). The synthesized beam is shown in the lower left hand corner.

IV. DISCUSSION

a) *Comparison with Infrared and Continuum Sources*

DR 21 and DR 21(OH) are part of an extended complex of star-forming regions, with numerous associated infrared and radio continuum sources, OH and H_2O masers, and dense

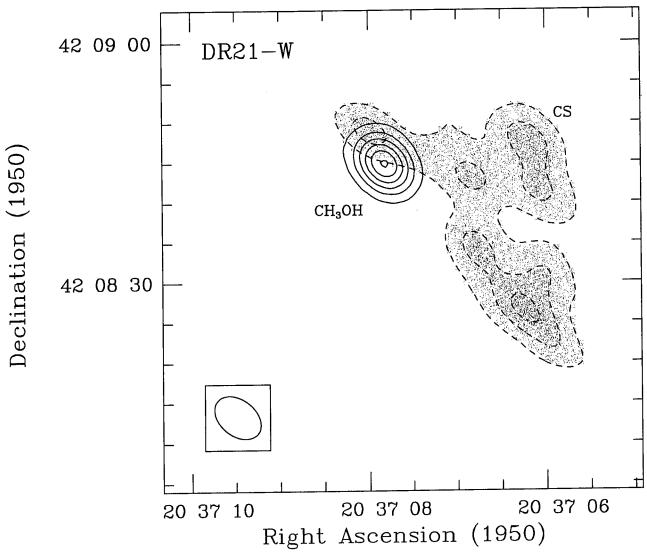

FIG. 4.—Comparison of CH_3OH $8_0 \rightarrow 7_1 A^+$ (*solid contours*) and CS $J = 2 \rightarrow 1$ (*dashed shaded contours*) integrated intensity maps toward DR 21. Contours are 75, 150, 225, 300, 375, and 450 K km s^{-1} for CH_3OH and 24, 48, and 72 K km s^{-1} for CS. Methanol maser DR 21-W corresponds to the methanol emission peak shown; maser DR 21-C is outside the box plotted. No extended thermal methanol emission was detected.

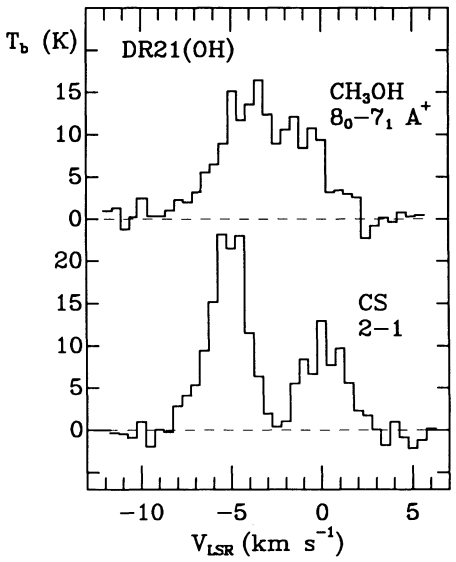

FIG. 5.—Spectra of thermal CH_3OH and CS emission seen toward $\alpha_{1950} = 20^h37^m14^s.11$, $\delta_{1950} = 42°12'08''$, midway between maser spots DR 21(OH)-2 and DR 21(OH)-4. The spectra were generated from maps with 0.5 km s^{-1} resolution, convolved with a 10″ × 5″ beam at position angle 30°.

molecular cores. As shown in Figures 1 and 6, we find that the 95 GHz methanol masers are offset from all these sources.

DR 21 consists of a cluster of compact H II regions distributed over an area of 20″ × 30″ or 0.3 pc × 0.4 pc at an assumed distance of 3 kpc (Roelfsema, Goss, and Geballe 1989). Several infrared sources (Wynn-Williams, Becklin, and Neugebauer 1974) and water masers (Genzel and Downes 1977) are detected in the vicinity of the H II regions, while luminous emission from shock-excited molecular hydrogen (H_2) extends ~2.5 pc east and west from the center (Garden *et al.* 1986). Although few existing molecular line observations have sampled the region ~1′ west of DR 21, where we find the intense DR 21-W maser, our aperture synthesis maps (Fig. 4) indicate that the methanol maser does not coincide with the CS emission peak in this direction. We have searched unsuccessfully for water maser emission toward DR 21-W using the Bonn 100 m telescope; a 3 σ upper limit on the water flux density of 0.3 Jy was determined on 1989 February 6.

A ridge of high-density molecular gas connects DR 21 with the OH maser/far-infrared source DR 21(OH) (Norris *et al.* 1982; Harvey, Campbell, and Hoffmann 1977), about 3′ north of DR 21. Several H_2O masers (Genzel and Downes 1977) are associated with DR 21(OH). High spatial resolution (sub-) millimeter continuum maps (Gear *et al.* 1988; Richardson, Sandell, and Krisciunas 1989; Woody *et al.* 1989) and interferometric observations of H_2CO and $C^{18}O$ emission (Johnston, Henkel, and Wilson 1984; Padin *et al.* 1989) show that DR 21(OH) consists of several dense clumps without associated radio continuum emission. Another infrared source, W75 IRS 1, is located ~1′ west of DR 21(OH) (Wynn-Williams, Becklin, and Neugebauer 1974) and also is surrounded by H_2 emission (Garden *et al.* 1986). Methanol masers 1–4 are not coincident with any of these sources.

b) Comparison with Other Methanol Transitions

Comparing our results with observations of other methanol transitions toward DR 21 and DR 21(OH), we find strong evidence that the 95 GHz $8_0 \rightarrow 7_1A^+$ masers originate in the same clumps of gas which produce $4_{-1} \rightarrow 3_0E$, $7_0 \rightarrow 6_1A^+$, $5_{-1} \rightarrow 4_0E$, and (in some cases) $J_2 \rightarrow J_1E$ methanol masers.

Methanol maser emission ~75″ west of the DR 21 continuum source was first detected by Menten *et al.* (1986) in the series GHz $J_2 \rightarrow J_1E$ ($J = 2, 3, 4, \ldots$) methanol lines. The position determined by Menten *et al.* (1986) for the $6_2 \rightarrow 6_1E$ maser is in excellent agreement with our DR 21-W maser position (see Fig. 6). Haschick, Menten, and Baan (1990) have detected maser emission in the 36 GHz $4_{-1} \rightarrow 3_0E$ and 44 GHz $7_0 \rightarrow 6_1A^+$ transitions in the same direction. The spectra of all these transitions are very similar, with an intense narrow spike at $v_{LSR} = -2.6$ km s^{-1} and low-level emission at higher velocities.

Toward DR 21 Menten *et al.* (1986) do not report any emission in the 25 GHz lines at a velocity of −3.5 km s^{-1}, corresponding to the DR 21-C maser velocity, but Bachiller *et al.* (1990) do detect a narrow −3.7 km s^{-1} emission feature in the $7_0 \rightarrow 6_1A^+$ transition. The absolute positions determined by Bachiller *et al.* (1990) for the −2.6 km s^{-1} and −3.7 km s^{-1} masers are too uncertain to allow conclusive identification with our DR 21-W and DR 21-C positions, but the ~85″

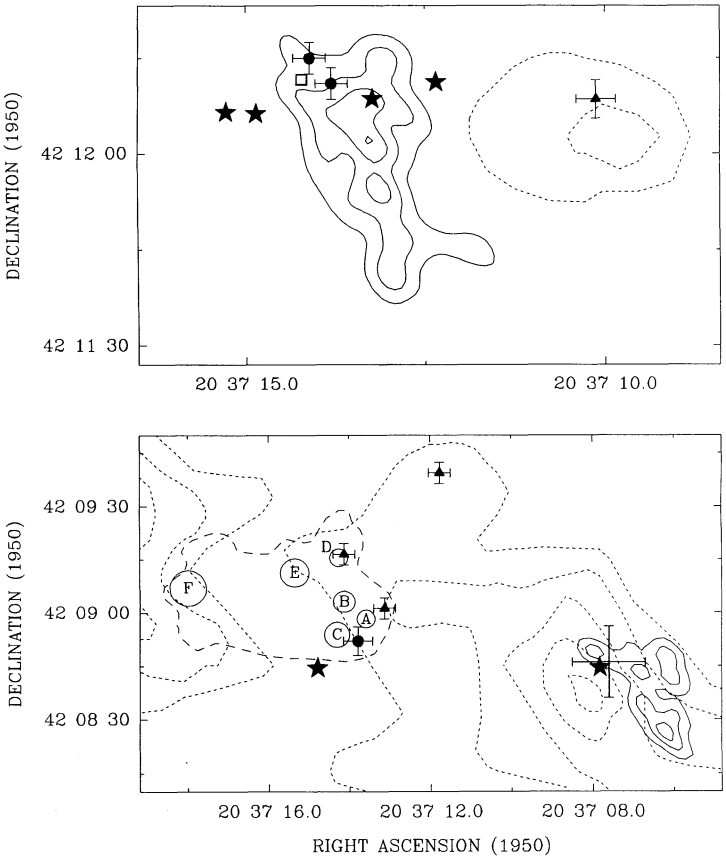

FIG. 6.—Enlarged views of the DR 21(OH) (*top*) and DR 21 (*bottom*) regions. Note that the two panels have different scales. Symbols are the same as the ones used in Fig. 1, except that the long dashes in the lower panel mark the extent of diffuse continuum emission surrounding DR 21 components A–F (in the nomenclature of Roelfsema, Goss, and Geballe 1989). Uncertainties in the IR and H_2O maser positions are indicated by error bars. Note that the stars denoting the methanol positions are considerably larger than the uncertainties of these positions (see Table 1). The error bar close to the western DR 21 methanol maser indicates the position determined by Menten *et al.* (1986) for the $6_2 \rightarrow 6_1E$ methanol maser.

separation they find between the two components is consistent with our value.

Toward DR 21(OH) the 25 GHz lines show (quasi-)thermal emission (Menten *et al.* 1986) with no obvious sign of maser action, while intense masers are observed in the $4_{-1} \rightarrow 3_0 E$, $7_0 \rightarrow 6_1 A^+$, and $5_{-1} \rightarrow 4_0 E$ transitions at 36, 44, and 84 GHz (Haschick and Baan 1989; Haschick, Menten, and Baan 1990; Batrla and Menten 1988). As in the case of DR 21, the maser spectra resemble each other very closely.

All of the 95 GHz maser spots that we identify in the DR 21(OH) field were previously detected in interferometric observations of the 84 GHz $5_{-1} \rightarrow 4_0 E$ transition by Batrla and Menten (1988). For convenience, we have numbered the spots 1–4 to correspond to Batrla and Menten's (1988) labeling scheme. Although Batrla and Menten (1988) attributed features 3 and 4 to thermal emission, the narrow line widths and relatively high brightness temperatures (~ 100 K at position 3) seen in the 95 GHz spectra suggest that these features also are masers. The absolute position we measure for the strong maser at position 1 differs from the position given by Batrla and Menten by only 0".35, less than the combined uncertainties of the two measurements, demonstrating that maser emission from the two transitions originates in the same volume of gas. Maser features 2–4 are located within 3" of the corresponding 84 GHz positions.

The 95 and 84 GHz line profiles measured toward each position are remarkably similar. The $8_0 \rightarrow 7_1 A^+$ rest frequency used by Batrla and Menten (1988) differs slightly from the very accurate value (84.521182 GHz) calculated recently by De Lucia *et al.* (1989), so all LSR velocities given by Batrla and Menten (1988) should be decreased by 0.10 km s^{-1}. This brings the 95 and 84 GHz LSR velocities into excellent agreement.

The observations of simultaneous maser emission in the $4_{-1} \rightarrow 3_0 E$, $7_0 \rightarrow 6_1 A^+$, $5_{-1} \rightarrow 4_0 E$, and $8_0 \rightarrow 7_1 A^+$ transitions provides an important clue to the physical conditions in the maser regions. Menten *et al.* (1990) have performed extensive statistical equilibrium calculations and find that collisional excitation of methanol can lead to simultaneous inversion of all these transitions for a methanol abundance of 10^{-7}, a kinetic temperature of 100 K, and densities of several $\times 10^4$ to 10^6 cm^{-3}.

c) *Methanol Masers and Outflows*

Inspection of Figure 6 shows that the brightest methanol masers, DR 21(OH)-1 and DR 21-W, are located *between* CS emission peaks and H_2 emission regions. Since CS emission originates from dense molecular gas, while H_2 emission traces shock fronts associated with outflows, this observation suggests that the interaction of outflows with dense clumps of gas may lead to the formation of methanol masers.

Since the maser velocities correspond to the ambient cloud velocities, the maser clumps apparently have not been accelerated by the outflow, like high-velocity water masers, but possibly have experienced substantial heating. Observations suggest that the fractional abundance of methanol $[n(CH_3OH)/n(H_2)]$ can be as high as 10^{-7}–10^{-6} in warm dense regions, up to 100 times greater than the methanol abundance in cold clouds (Menten *et al.* 1986, 1988). Such overabundances may be explained by the evaporation of methanol ice condensed on dust grains (Menten *et al.* 1988), by chemical reactions taking place in the interaction regions between outflows and ambient molecular cloud gas (Blake *et al.* 1987; Plambeck and Wright 1988), or by a combination of these processes.

Recently Elitzur, Hollenbach, and McKee (1989) have presented a model for H_2O masers in star-forming regions. In their scheme, H_2O masers are formed in warm (~ 400 K) dense (10^9 cm^{-3}) postshock gas behind high-velocity (≥ 50 km s^{-1}) shock fronts. Class A methanol masers cannot form in such an environment, since maser action in the observed transitions is quenched at densities $> 10^7$ cm^{-3}. The temperature requirements for the production of class A methanol masers also are much less stringent than for H_2O masers, since the upper state energies of the observed class A transitions are less than 150 K above the ground state, versus 643 K for the $6_{16} \rightarrow 5_{23}$ transition of H_2O.

Our results suggest that the methanol masers originate from relatively low mass clumps, making the nondetection of thermal emission from their locations understandable. The pedestal emission features associated with the masers apparently are unresolved by our beam, and so are less than about 2" (0.03 pc) in diameter, while the hydrogen densities must be less than 10^7 cm^{-3} in order not to quench the masers. The mass of such a clump is less than 7 $M_\odot$, far below the detection limits of the 800/1100 μm measurements of Richardson, Sandell, and Krisciunas (1989) for all reasonable values of the dust temperature.

V. SUMMARY

We mapped simultaneously the 95 GHz $8_0 \rightarrow 7_1 A^+$ transition of methanol and the 98 GHz $J = 2 \rightarrow 1$ transition of CS with 5" resolution toward DR 21(OH) and toward a position 1'.1 west of DR 21. We identify four methanol masers in the DR 21(OH) field and two masers in the DR 21 field. The masers are offset from known infrared and radio continuum sources and from OH and H_2O masers. They appear to lie on the periphery of dense molecular cores traced by CS emission.

All available evidence suggests that the $8_0 \rightarrow 7_1 A^+$ masers originate from the same clumps of gas responsible for maser emission in the $4_{-1} \rightarrow 3_0 E$, $7_0 \rightarrow 6_1 A^+$, $5_{-1} \rightarrow 4_0 E$, and $J_2 \rightarrow J_1 E$ methanol transitions. Comparisons of the DR 21(OH) masers with those previously mapped interferometrically in the $5_{-1} \rightarrow 4_0 E$ line are particularly convincing: the positions are coincident within 3" (within 0".35 for the strongest feature), and the LSR velocities and line shapes are in excellent agreement.

We argue that the methanol masers may be formed where molecular outflows shock preexisting dense clumps. Heating in such shocks can lead to an increased methanol abundance, favoring the formation of collisionally pumped methanol masers.

This work was supported in part by NSF grant AST 87-14721.

REFERENCES

Bachiller, R., Menten, K. M., Gómez-González, J., and Barcia, A. 1990, *Astr. Ap.*, in press.
Batrla, W., Matthews, H. E., Menten, K. M., and Walmsley, C. M. 1987, *Nature*, **326**, 49.
Batrla, W., and Menten, K. M. 1988, *Ap. J. (Letters)*, **329**, L117.
Blake, G. A., Sutton, E. C., Masson, C. R., and Phillips, T. G. 1987, *Ap. J.*, **315**, 621.
De Lucia, F. C., Herbst, E., Anderson, T., and Helminger, P. 1989, *J. Molec. Spectrosc.*, **134**, 395.
Elitzur, M., Hollenbach, D. J., and McKee, C. F. 1989, *Ap. J.*, **346**, 983.

Garden, R., Geballe, T. R., Gatley, I., and Nadeau, D. 1986, *M.N.R.A.S.*, **220**, 203.
Gear, W. K., Chandler, C. J., Moore, T. J. T., Cunningham, C. T., and Duncan, W. D. 1988, *M.N.R.A.S.*, **231**, 47p.
Genzel, R., and Downes, D. 1977, *Astr. Ap. Suppl.*, **30**, 145.
Harvey, P. M., Campbell, M. F., and Hoffmann, W. F. 1977, *Ap. J.*, **211**, 786.
Haschick, A. H., and Baan, W. A. 1989, *Ap. J.*, **339**, 949.
Haschick, A. H., Menten, K. M., and Baan, W. A. 1990, *Ap. J.*, **354**, 556.
Johnston, K. J., Henkel, C., and Wilson, T. L. 1984, *Ap. J. (Letters)*, **285**, L85.
Johnston, K. J., *et al.* 1990, in preparation.
Matsakis, D. N., Cheung, A. C., Wright, M. C. H., Askne, J. I. H., Townes, C. H., and Welch, W. J. 1980, *Ap. J.*, **236**, 481.
Menten, K. M., *et al.* 1990, in preparation.
Menten, K. M., Walmsley, C. M., Henkel, C., and Wilson, T. L. 1986, *Astr. Ap.*, **157**, 318.
———. 1988, *Astr. Ap.*, **198**, 253.
Norris, R. P., Booth, R. S., Diamond, P. J., and Porter, N. D. 1982, *M.N.R.A.S.*, **201**, 191.
Padin, S., *et al.* 1989, *Ap. J. (Letters)*, **337**, L45.
Plambeck, R. L., and Wright, M. C. H. 1988, *Ap. J. (Letters)*, **330**, L61.
Richardson, K. J., Sandell, G., and Krisciunas, K. 1989, *Astr. Ap.*, **224**, 199.
Roelfsema, P. R., Goss, W. M., and Geballe, T. R. 1989, *Astr. Ap.*, **222**, 247.
Woody, D. P., *et al.* 1989, *Ap. J. (Letters)*, **337**, L41.
Wynn-Williams, C. G., Becklin, E. E., and Neugebauer, G. 1974, *Ap. J.*, **187**, 473.

K. M. MENTEN: Harvard-Smithsonian Center for Astrophysics, 60 Garden Street, Cambridge, MA 02138

R. L. PLAMBECK: Radio Astronomy Laboratory, University of California, Berkeley, CA 94720